A Molecular Model for Axon Guidance Based on Cross Talk between Rho GTPases

Yuichi Sakumura,* Yuki Tsukada,* Nobuhiko Yamamoto,† and Shin Ishii*
*Graduate School of Information Science, Nara Institute of Science and Technology, 8916-5 Takayama, Ikoma, Nara 630-0192, Japan; and †Graduate School of Frontier Biosciences, Osaka University, 1-3 Yamadaoka, Suita, Osaka 565-0871, Japan

ABSTRACT To systematically understand the molecular events that underlie biological phenomena, we must develop methods to integrate an enormous amount of genomic and proteomic data. The integration of molecular data should go beyond the construction of biochemical cascades among molecules to include tying the biochemical phenomena to physical events. For the behavior and guidance of growth cones, it remains largely unclear how biochemical events in the cytoplasm are linked to the morphological changes of the growth cone. We take a computational approach to simulate the biochemical signaling cascade involving members of the Rho family of GTPases and examine their potential roles in growth-cone motility and axon guidance. Based on the interactions between Cdc42, Rac, and RhoA, we show that the activation of a Cdc42-specific GEF resulted in switching responses between oscillatory and convergent activities for all three GTPases. We propose that the switching responses of these GTPases are the molecular basis for the decision mechanism that determines the direction of the growth-cone expansion, providing a spatiotemporal integration mechanism that allows the growth cone to detect small gradients of external guidance cues. These results suggest a potential role for the cross talk between Rho GTPases in governing growth-cone movement and axon guidance and underscore the link between chemodynamic reactions and cellular behaviors.

INTRODUCTION

As exemplified by the development of thalamocortical and retinotectal projections, precisely coordinated pathfinding signals guide growing axons to their targets, allowing the axons to make specific synaptic connections in the developing nervous system (1,2). This precise construction of neural networks is crucial for carrying out brain functions. Previous studies on axon guidance have provided a wealth of information about guidance factors, their receptors, and cytoplasmic effectors (3–5). A theoretical study that explained the high sensitivity of cellular chemotaxis to molecule gradients, suggested that local activators and global inhibitors amplify a small gradient by a self-enhancing process (6,7). A recent theoretical study showed gradient detection by growth cones using a filopodia-generation mechanism (8). It is still unknown, however, how cellular signaling networks are coupled to growth-cone morphology and gradient detection.

As an axon develops, a growth cone changes its shape by reorganizing actin filaments depending on the type and concentration of external signals (9,10). Rho-family small GTPases, Cdc42, Rac, and RhoA, are important signaling molecules within growth cones, and are well-known regulators of actin polymerization in both nonneuronal cells and neuronal growth cones (11,12). During axon guidance, it is presently thought that: i), external signals (e.g., netrin) are integrated into the intracellular signaling cascade via membrane receptors; ii), these signals interact with GTPases (Cdc42, Rac, and RhoA), which also cross talk with each other; and iii), the resultant signals from the GTPases regulate cytoskeleton dynamics. The resulting phenomena include filopodia elongation mediated by Cdc42 activation, lamellipodia expansion after Rac activation, RhoA-mediated myosin phosphorylation and subsequent filopodia and lamellipodia retraction, and depolymerization of actin filaments, which is inhibited by these three GTPases (Fig. 1 *A*).

Thus, the network of Rho-family small GTPases is thought to be a computational system that translates external signals into the regulation of growth-cone movement and axon guidance (13). In addition, the mechanics of axon guidance and the morphological changes in growth cones are prototypical examples of microscopic molecular interactions resulting in macroscopic biological functions and cellular morphologies. In this study, we first examine the qualitative characteristics of the GTPase cross talk. We show that the GTPase activities can exhibit switching responses as a result of variations in the exogenous guanine nucleotide exchange factors (GEFs). Second, we propose a computational model for the molecular machinery, in which cross talk between Rho-family small GTPases induces growth-cone movement and chemoattractive axon guidance. Our model implies that the GTPase switching response plays a significant role in axon guidance and that local nonlinearity in the GTPase responses, rather than localization of GEF signals, is important for gradient detection. Finally, we explore possible or significant cascades in the GTPase cross talk by the Monte Carlo method and give predictive suggestions about characteristics of the kinetics.

Submitted November 3, 2004, and accepted for publication May 2, 2005.

Address reprint requests to Shin Ishii, E-mail: ishii@is.naist.jp.

0006-3495/05/08/812/11 $2.00

doi: 10.1529/biophysj.104.055624

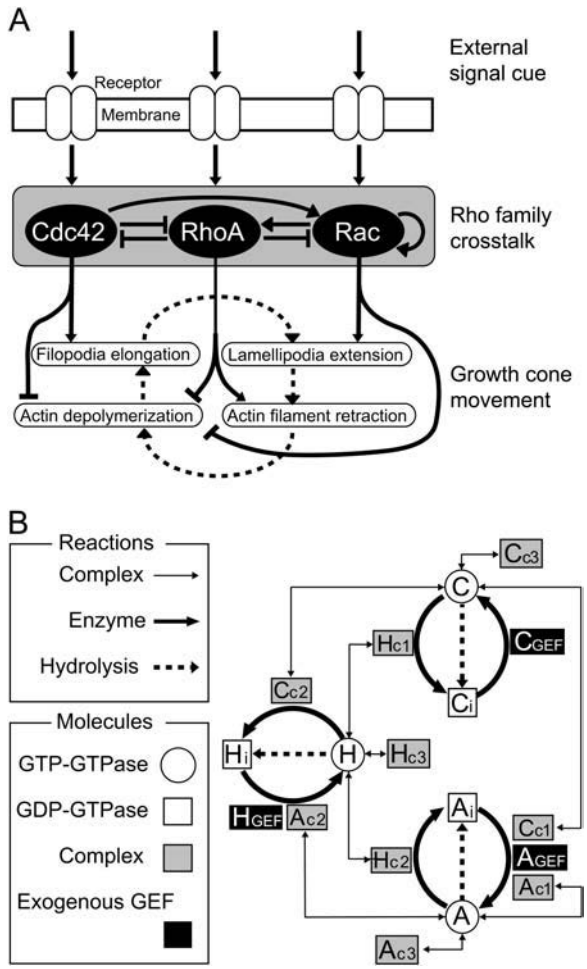

FIGURE 1 Possible signaling pathways and activation characteristics in a model growth cone. (*A*) A diagram depicting the signaling cascade from the external cue molecules to growth-cone behavior including the cross talk between the GTPases (Cdc42, Rac, and RhoA). Cdc42 activates actin polymerization in the tips of filopodia, Rac activates actin polymerization for lamellipodia at cell membranes, RhoA activates actin filament retraction by phosphorylating myosin, and all three proteins inhibit actin depolymerization in a growth cone. (*B*) A speculative biochemical signaling cascade of GTPase cross talk. Each GTPase can assume three different states: a GDP-bound inactive state, a GTP-bound active state, and a complex state that consists of a GTP-bound GTPase and other proteins. *C*, *A*, and *H* are the amount of active Cdc42, Rac, and RhoA (GTP-bound), respectively. The variables with suffix *i* denote the proteins in an inactive state (GDP-bound), whereas *c*1, *c*2, and *c*3 signify those in complex states. The complexes with the suffixes *c*1 and *c*2 are enzymes, whereas the complex with the *c*3 suffix governs a downstream event such as actin polymerization. GTP-bound GTPases hydrolyze the bound nucleotide at a constant rate (h_C, h_A, and h_H), thereby becoming GDP-bound proteins. GAPs increase the rate of GTP hydrolysis, whereas GDP for GTP exchange is facilitated by GEFs. Each of the exogenous GEF concentrations (C_{GEF}, A_{GEF}, and H_{GEF}) varies depending on diffusion, degeneration, and the reaction to external molecular cues. The GTP-bound Cdc42 forms a complex (C_{c1}) with other proteins, and becomes a GEF enzyme for Rac. Similarly, the GTP-bound Rac turns into a GEF enzyme for itself. Accordingly, some of the interactions depicted in this figure have been experimentally observed. It has been previously reported that GTP-bound Cdc42 binds to PAK and Pix/Cool (34) and becomes a GEF enzyme for Rac. Plexin B (19) is thought to sequester GTP-bound Rac, while at the same time acting as a GEF enzyme for RhoA.

METHODS AND RESULTS

The kinetics of cross talk between Rho GTPases

Cross talk between GTPases was first reported in fibroblasts, in which Cdc42 activates Rac, Rac activates RhoA, Cdc42 and RhoA mutually inhibit each other, and RhoA inhibits Rac (14,15). These observations can be consolidated into the signaling cascade illustrated in Fig. 1 *B* in which GTPases can exist in three states: activated, inactivated, and complex. The transition from an inactive state to an active state is mediated by GEFs, whereas GTP hydrolysis is promoted by the activity of GTPase-activating proteins (GAPs) (11,12,16,17,18,19). It is thought that the active form of each of these three G-proteins makes a complex with other proteins, thereby enabling them to act as either a GEF or a GAP. In other words, GTP-bound active GTPases form complexes with other proteins and enzymatically act on other GTPases and/or themselves.

The complex processes and the enzymatic reactions involved in GTPase cross talk can be expressed as the following molecule-molecule interactions and enzymatic reactions:

$$\mathrm{B} + \mathrm{G}^* \rightleftharpoons \mathrm{BG}^*$$
$$(\mathrm{BG}^*) + \mathrm{G} \rightleftharpoons (\mathrm{BG}^*) \cdot \mathrm{G} \rightarrow (\mathrm{BG}^*) + \mathrm{P},$$

where G^* is an active GTPase (GTP-GTPase) that binds an effector molecule, B, to form the complex BG^*. A GTPase (G) is transformed into a product (P, a GTP- or GDP-bound GTPase) by the enzyme BG^*. During the enzymatic reactions, a vast excess of the substrate ($[BG^*] \ll [G]$) and steady-state conditions ($d[(BG^*) \cdot G]/dt = 0$) can be commonly assumed. This leads to the additional assumption that the reaction $B + G^* \rightleftarrows BG^*$ is also in a steady state ($d[BG^*]/dt = 0$) because the amount of the enzyme, BG^*, is much smaller than the amount of G^*. Thus, the overall rate of the GTPase reactions is dominated by the process $(BG^*) \cdot G \rightarrow (BG^*) + P$.

In the signaling cascade depicted in Fig. 1 *B*, we can write the ordinary equations for the complex of Cdc42 as follows:

$$\frac{dC_{c1}}{dt} = k_1^+ C - k_1^- C_{c1}$$
$$\frac{dC_{c2}}{dt} = k_2^+ C - k_2^- C_{c2}$$
$$\frac{dC_{c3}}{dt} = k_3^+ C - k_3^- C_{c3},$$

where t is the time (in seconds) and the parameters k_j^+ and k_j^- $(j = 1, 2, 3)$ are the rate constants for the forward and backward reactions, respectively. Using the steady-state conditions

Finally, it is thought that GTP-bound Rac can act as a GAP for RhoA, the GTP-bound RhoA can act as a GAP for Cdc42 and Rac, and GTP-bound Cdc42 can act as a GAP for RhoA; these activation and inactivation relationships have been empirically observed.

of the molecule-molecule reactions ($dC_{cj}/dt = 0$), the three complex states can be written as $C_{cj} = k_j C = (k_j^+/k_j^-)C$ ($0 < k_j < 1$, $j = 1, 2, 3$). For the inactive state (C_i), with normalization for the total quantity of Cdc42, $C_i + C + C_{c1} + C_{c2} + C_{c3} = 1$, we obtain $C_i = 1 - \rho_C C$, where $\rho_C = 1 + k_1 + k_2 + k_3$. Similarly, we can write $A_{cj} = l_j A$, $A_i = 1 - \rho_A A$, $H_{cj} = m_j H$, and $H_i = 1 - \rho_H H$ with conditions $l_j = l_j^+/l_j^-$, $\rho_A = 1 + l_1 + l_2 + l_3$ ($0 < l_j < 1.0, j = 1, 2, 3$) for Rac, and $m_j = m_j^+/m_j^-$ and $\rho_H = 1 + m_1 + m_2 + m_3$ ($0 < m_j < 1.0, j = 1, 2, 3$) for RhoA.

The active state of Cdc42 (C) increases with the exchange of GTP for GDP by the inactive state (C_i) and via the backward reactions from the complex states (C_{c1}, C_{c2}, and C_{c3}), and is decreased by GTP hydrolysis and the synthesizations. Then, the ordinary differential equation for the activation of Cdc42 is

$$\frac{dC}{dt} = \frac{k^- C_{GEF} C_i}{K_m^- + C_i} + k_1^- C_{c1} + k_2^- C_{c2} + k_3^- C_{c3} - \frac{k^+ H_{c1} C}{K_m^+ + C} - (h_C + k_1^+ + k_2^+ + k_3^+)C, \quad (1)$$

where h_C is the rate of hydrolysis for GTP-bound Cdc42 and H_{c1} is the amount of GAP enzyme that is synthesized from the active state of RhoA (H). Enzymatic reactions were modeled by the Michaelis-Menten formula with Michaelis constants, K_m^- and K_m^+ (normalized concentration), and catalytic constants, k^- and k^+ (s^{-1}). Similarly, for Rac and RhoA, we obtain:

$$\frac{dA}{dt} = \frac{l^-(C_{c1} + A_{c1} + A_{GEF})A_i}{L_m^+ + A_i} + l_1^- A_{c1} + l_2^- A_{c2} + l_3^- A_{c3} - \frac{l^+ H_{c2} A}{L_m^- + A} - (h_A + l_1^+ + l_2^+ + l_3^+)A \quad (2)$$

$$\frac{dH}{dt} = \frac{m^-(A_{c2} + H_{GEF})H_i}{M_m^- + H_i} + m_1^- H_{c1} + m_2^- H_{c2} + m_3^- H_{c3} - \frac{m^+ C_{c2} H}{M_m^+ + H} - (h_H + m_1^+ + m_2^+ + m_3^+)H, \quad (3)$$

where L_m^-, L_m^+, M_m^-, and M_m^+ are Michaelis constants (normalized concentration) and l^-, l^+, m^-, and m^+ (s^{-1}) are catalytic constants; h_A and h_H are the constant rates of hydrolysis of GTP by activated Rac and RhoA (20). By applying the steady-state conditions, Eqs. 1–3 become:

$$\frac{dC}{dt} = \frac{k^- C_{GEF}(1 - \rho_C C)}{K_m^- + 1 - \rho_C C} - \frac{k^+ m_1 H C}{K_m^+ + C} - h_C C \quad (4)$$

$$\frac{dA}{dt} = \frac{l^-(k_1 C + l_1 A + A_{GEF})(1 - \rho_A A)}{L_m^- + 1 - \rho_A A} - \frac{l^+ m_2 H A}{L_m^+ + A} - h_A A \quad (5)$$

$$\frac{dH}{dt} = \frac{m^-(l_2 A + H_{GEF})(1 - \rho_H H)}{M_m^- + 1 - \rho_H H} - \frac{m^+ k_2 C H}{M_m^+ + H} - h_H H. \quad (6)$$

We examined the characteristics of GTPase cross talk using these three equations.

Characteristics of the kinetics

Although the signals that transduce the external cues to the GTPase network are becoming clear (21), most of the chemical parameters remain unknown. Because many of the reaction coefficients in Fig. 1 *B* are also unknown, we allocated a number of possible parameter sets to qualitatively analyze the kinetics of these reactions. The inverse values of the dissociation constants (e.g., k_1, l_2, and m_2) were systematically prepared as discrete values ranging from [0.01,0.30], by considering the condition that the levels of the complex states (e.g., C_{c1}) should be smaller than the levels of the active state (e.g., C). The values of Michaelis constants (e.g., K_m^-, L_m^+, and M_m^-) were from [0.01,0.50] (normalized concentration), which is an appropriate range because the active state variables C, A, and H were normalized to be 1.0. Catalytic constants (e.g., k^+, l^-, and m^+) ranged from [0.1,0.9] (s^{-1}), values that approximated experimentally measured constants (22). The concentrations of the three exogenous GEFs (e.g., C_{GEF}, A_{GEF}, and H_{GEF}), which are generated downstream of the external cue molecules, were varied from [0.01,0.30], and the concentrations of the corresponding enzymes ranged from [0.003,0.09] if the average activity of a single GTPase was 0.3. According to the Monte Carlo parameter allocation (see the section ''Reaction coefficients for oscillation'' and Fig. 6), the kinetic responses to various exogenous GEF concentrations could be classified as either oscillatory or convergent.

Because we most frequently observed a switching response between oscillatory and convergent when the level of the exogenous Cdc42-GEF was varied (Fig. 6), we show GTPase responses to changes in the exogenous Cdc42-GEF concentration (C_{GEF}) as representatives of the oscillatory responses (Fig. 2). When C_{GEF} was increased from zero while the other parameters were fixed (Table 1), the activity of the Rac complex (A_{c3}) dramatically switched from converging to oscillating in an ultrasensitive manner (Fig. 2 *A*). This oscillatory activity spontaneously occurred due to the mutual GTPase interactions if exogenous Cdc42-GEF was continuously supplied. The amount of GTPase in a complex state oscillated with a fixed temporal order (Cdc42 → Rac → RhoA) (Fig. 2 *B*). The temporal order of the activity peaks of Cdc42, Rac, and RhoA did not vary regardless of the applied parameters because this activity stream originated from the signaling pathway, in which Cdc42 activates Rac, Rac activates RhoA, and RhoA inactivates Cdc42. Biochemical oscillations have frequently been observed in the activities of intracellular signaling pathways (23). It is possible that the steady-state conditions assumed in the kinetic model (e.g., $dC_{cj}/dt = 0$) allow the GTPase activity to oscillate. To test the GTPase oscillations in the absence of the steady-state conditions, we also simulated the GTPase cross talk, using a GENESIS simulator with a Kinetikit interface (24). This simulation included molecule-molecule interactions such as protein syntheses (e.g., PAK/Cdc42 complex). We found

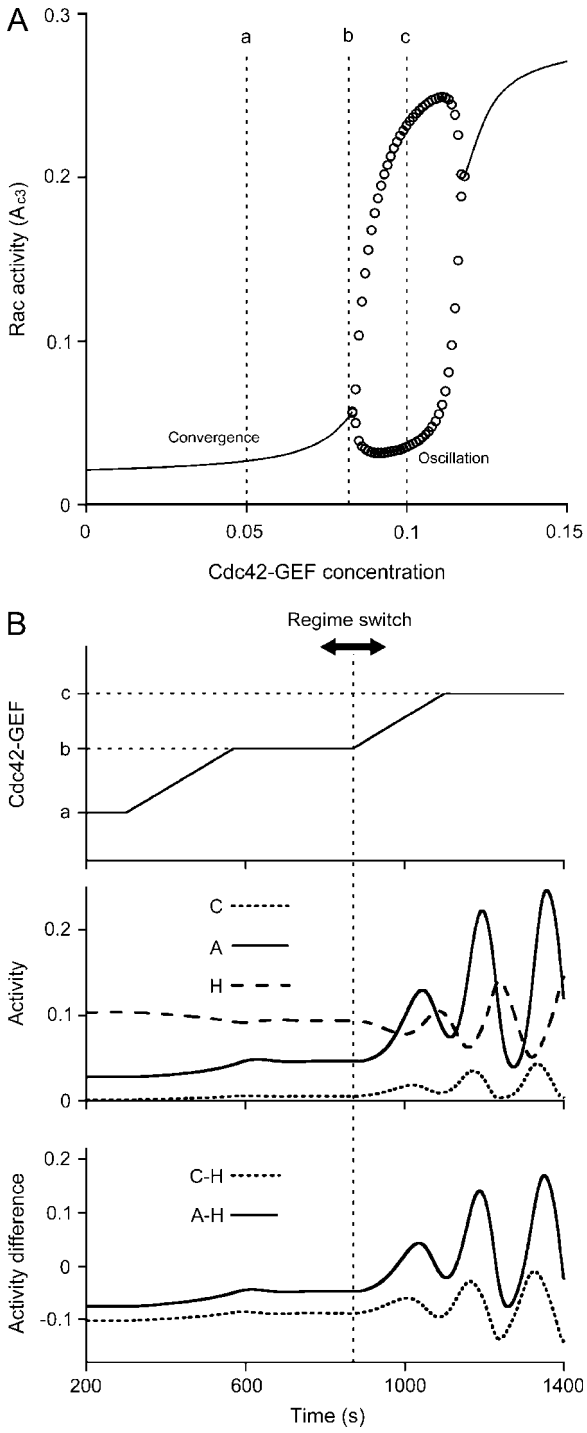

FIGURE 2 The switching response due to the GTPase cross talk. (*A*) Characteristics of a complex state of Rac GTPase (A_{c3}) are plotted against the supplied Cdc42-GEF concentration (C_{GEF}). The complex activity shows the switching response between convergence (*solid curves*) and oscillation (*upper circles* are maximums and *lower circles* are minimums). Concentration values at *a*, *b*, and *c* represent the system during convergence (0.05), at the boundary between convergence and oscillation (0.083), and during oscillation (0.1), respectively. We assume that this activity becomes an upstream signal for the cytoskeletal dynamics, and that the switching-like signal also propagates downstream. (*B*) Time courses of the Cdc42-GEF concentration (*top*), the resultant activities of the complexes of Cdc42 (C_{c3}), Rac (A_{c3}), and RhoA (H_{c3}) (*middle*), and the activity differences, $C_{c3} - H_{c3}$ and $A_{c3} - H_{c3}$ (*bottom*). The Cdc42-GEF concentrations *a*, *b*, and *c* are the same as those in panel *A*. Reaction parameters are listed in Table 1.

that the GTPase cross talk without assuming the steady-state conditions exhibited oscillatory responses (data not shown).

Growth-cone model

Although an axon normally elongates along a straight path, it can suddenly change the direction of its migration. For example, a concentration gradient of a cue molecule can provoke a zigzag pattern of elongation (25). It is likely that one of the functions of the growth cone is to control axonal turning and that the activities of intracellular molecules change (switching) to turn the axon toward a different direction.

It is reasonable to assume that the nonlinear and ultrasensitive change (switch) accompanying the oscillation of the local GTPase activity reflects the growth-cone motility. The change of the neurite shape strongly correlates with local GTPase activity, which has a timescale of a few minutes (26). Moreover, the time constants for oscillatory actin dynamics and myosin activity can be estimated to be ~100 s (27), which is in the same range as the timescale of the GTPase enzyme reaction (Fig. 2 *B*). Considering the fact that GTPases activate LIM kinase, which phosphorylates and inactivates cofilin, an actin-depolymerization factor (28–30), the temporal order of the GTPase activities (Cdc42 → Rac → RhoA; Fig. 2 *B*) regulates the movement of the cytoskeleton as follows: polymerization of actin filaments in filopodia and lamellipodia, actin filament retraction, and an increase in the number of actin monomers due to low GTPase activities. This cytoskeletal cycle can generate an effective expansion of the growth cone. When a forcing oscillation, such as a GTPase oscillation, has a similar period to its responding oscillation, such as the actin cycle, the responding oscillation could be entrained into the forcing oscillation, making that growth-cone expansion stable, because the reaction delay between the GTPase oscillation and the cytoskeletal oscillation may be essentially unchangeable.

We hypothesize that the ultrasensitive switching from a convergent state to an oscillatory state works to switch two qualitatively different modes of elongation during axon guidance: straight elongation and sudden turning. We believe that the growth cone will progress along a straight path while the GTPase activities are in a convergent state, whereas large turns are induced by oscillations of their activities; the ultrasensitivity of the system largely expands the oscillation amplitude, which locally encourages the expansion. One may consider the possibility that the effective expansion is achieved with, for example, low constant RhoA activity and high constant activities of Cdc42 and Rac. In this

TABLE 1 Parameter values used in Fig. 2

GTPase	Meaning						
Cdc42							
	1/Dissociation constant	k_1	0.1	k_2	0.9	k_3	0.2
	Catalytic constant*	k^+	0.4	k^-	0.4	–	–
	Michaelis constant	K_m^+	0.40	K_m^-	0.01	–	–
Rac							
	1/Dissociation constant	l_1	0.4	l_2	0.1	l_3	0.8
	Catalytic constant*	l^+	0.2	l^-	0.6	–	–
	Michaelis constant	L_m^+	0.15	L_m^-	0.22	–	–
RhoA							
	1/Dissociation constant	m_1	0.6	m_2	0.3	m_3	0.8
	Catalytic constant*	m^+	0.5	m^-	0.3	–	–
	Michaelis constant	M_m^+	0.34	M_m^-	0.39	–	–

Rates of hydrolysis $h_C = h_A = h_H = 0.03$ (20) and GEFs are $A_{GEF} = H_{GEF} = 0.01$.
*Experimental measurements are in the range [0:1.0] (s^{-1}) (22).

constant activity regime, however, it is difficult for the growth cone to turn with a large angle due to the absence of the mechanism that governs changes in the direction of expansion. In addition, because we could not find reaction parameters with which the GTPase cross talk showed nonlinear Rac activity in response to an increase of exogenous GEFs, the GTPase switching response between convergence and oscillation is necessary to change the expansion direction (see below).

Winner-takes-direction model

We postulated that the GTPase-activity switch is the threshold mechanism that produces a new growth cone between two filopodia because the oscillations of actin polymerization and filament retraction amplify the expansion of the growth cone (suprathreshold, jumping-expansion mode) more than in the convergent condition (subthreshold, normal expansion mode). The switching response between these expansion modes due to the exogenous GEFs (C_{GEF} for example) is the primary means by which the model growth cone can initiate the turning mechanism (winner-takes-direction model).

The model growth cone we used had six filopodia ($M = 6$), which are radially and equiangularly distributed with an interval 22.5° ($\pi/8$ rad) around the lamellipodia (Fig. 3 *A*). The length of each filopodium and the radius of each lamellipodium were both set to 1 (normalized length). The model growth cone spatially and temporally integrated external cue molecules and grew in the direction along which its lamellipodia expanded. The growing process of the model growth cone assumed the following two things. First, if all the lamellipodia were in the normal expansion mode, the growth direction and length were defined as the vector summation of the lamellipodia expansions (see ''Lamellipodia expansion'' below). In this case, the coordinate vector of the center of the growth cone at time t, $\vec{X}(t)$, transfers to $\vec{X}(t+\Delta t) = \vec{X}(t)+\Delta\vec{X}(t)$, where $\Delta\vec{X}(t)$ is the sum of the expansion vectors of the five lamellipodia (see below, Eq. 8). Second, because lamellipodia in the jumping-expansion mode consumed a large fraction of the available actin monomers while depriving other filopodia and lamellipodia of these subunits, the lamellipodium that first reached the jumping-expansion mode, produced a new growth cone while at the same time the old growth cone retrogressed (*middle* and *right* panels in Fig. 3 *A*). This lamellipodium expansion was based on experimental observations (10,31). After either of these two types of axonal progress (normal or jumping), the cone was able to again integrate external cues.

Lamellipodia expansion

Considering the complex state of the Rac GTPase (A_{c3}) in Fig. 2, the expansion rate function of a single lamellipodium in the normal expansion mode is represented as a monotonically increasing function (Fig. 3 *B*). This function corresponds to the convergent behavior observed for the Rac complex with small C_{GEF} values (Fig. 2). Therefore, the expansion rate function is expressed as $G_{i,i+1}/10^6$ if $G_{i,i+1} \le \theta_{th}$, where the parameter θ_{th} is the threshold value (=15), which is 150 times larger than the GEF concentration generated by a single cue molecule. $G_{i,i+1}$, the integrated concentration of the GEF within the lamellipodium between the ith and the $(i+1)$th filopodia ($1 \le i \le M-1 = 5$), is written as:

$$G_{i,i+1} = \frac{K_i + K_{i+1}}{3} + \frac{K_{i-1} + K_{i+2}}{6} + G, \qquad (7)$$

where G (an intrinsic GEF) has a constant value of 1.0 and K_i is the temporal summation of the amount of the GEF multiplied by the spatial attenuation ($E_i(t)A_i(D)$; see ''Exogenous GEF'') induced by the ith filopodium. The boundary condition is $K_0 = K_7 = 0$. This equation models the spatial redistribution of GEF molecules among the four nearest filopodia. In the normal expansion mode, the vector summation, $\Delta\vec{X}(t)$, is expressed as follows:

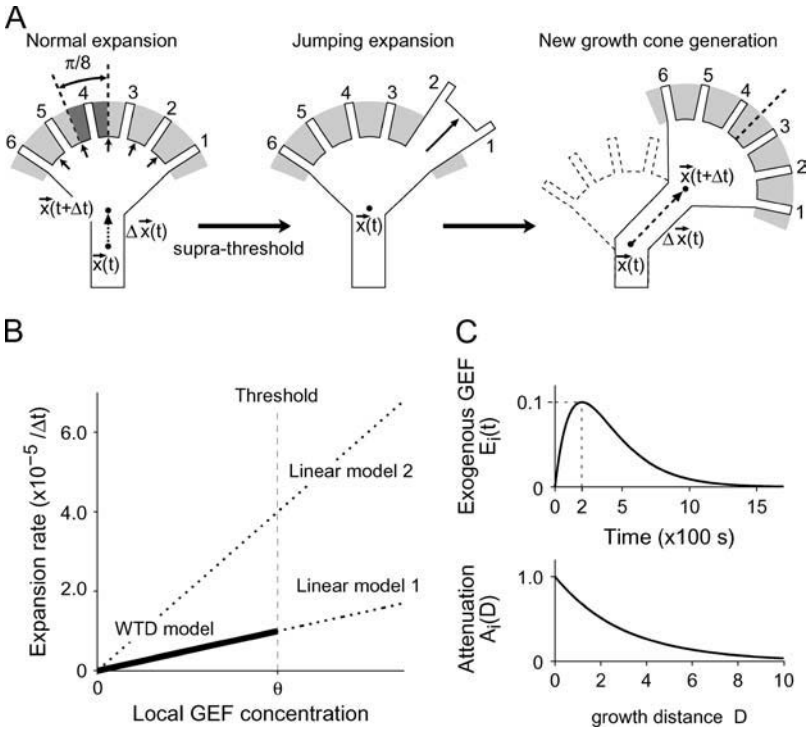

FIGURE 3 A schematic diagram of the growth-cone model. (*A*) A sketch of the winner-takes-direction (*WTD*) model. A model growth cone has six filopodia and five semicircular lamellipodia. The model assumes that each filopodium can detect external cue molecules within $\pm\pi/8$ (rad) around the filopodium (*dark gray* region in the *left* panel), serving cue detection on the neighboring lamellipodia. In this way, cue molecules in the entire light gray region can be detected. When the local GEF concentration between filopodium 1 and filopodium 2 reaches a specific threshold (*middle* panel), the lamellipodium between these filopodia performs a jumping expansion (*right* panel). After the jumping expansion, the model growth cone extends new filopodia and lamellipodia with the lamellipodium that executed the jumping expansion positioned in the center of the growth cone (between filopodium 3 and filopodium 4). (*B*) The lamellipodium expansion rate plotted against the local spatiotemporal summation of the level of GEF in a single lamellipodium. The thick solid line represents the expansion rate in the WTD model, whereas the thin dotted lines represent of the expansion rates in two linear expansion models (no threshold). (*C*) $E_i(t)$, which represents the amount of exogenous GEFs generated downstream of external single cue molecules detected by the *i*th filopodium, is modeled as a time-dependent function (*top*). We assume the efficiency is attenuated with growth distance, *D*. This attenuation rate is expressed as an exponential function, $A_i(D)$ (*bottom*).

$$\Delta\vec{X}(t) = \sum_{i=1}^{5} F_{ex}(G_{i,i+1}) \times \vec{e}_{i,i+1}, \tag{8}$$

where $F_{ex}(x)$ is the expansion rate function (Fig. 3 *B*) and $\vec{e}_{i,i+1}$ is a unit vector that is parallel to the direction of the lamellipodium between the *i*th and the $(i+1)$th filopodia.

For growth-cone production, it is assumed that the amount of GEF ($G_{i,i+1}$) in the lamellipodium in the jumping-expansion mode is redistributed by initializing K_i values to $K_3 = K_4 = G_{i,i+1}/3$, $K_2 = K_5 = G_{i,i+1}/6$, and $K_1 = K_6 = 0$. This redistribution process of GEF molecules restricts the concentration to very low values so that the GTPase activities cannot shift from oscillatory to convergent (the right convergent region in Fig. 2 *A*).

Exogenous GEF

Guidance cue molecules are captured by receptors on the membrane. The receptors translate the external cue signals into intracellular reactions. The local activation of exogenous GEF in the model growth cone was assumed to exhibit a time-dependent change due to autonomous protein synthesis and degeneration ($E_i(t)$). The GEF activity was also attenuated as the growth cone extended ($A_i(D)$) because the position of the receptor upstream of this GEF was fixed. These temporal and spatial effects are expressed as

$$E_i(t) = \frac{t}{\tau_{decay}} exp\left(1 - \frac{t}{\tau_{decay}}\right)$$

$$A_i(D) = exp\left(-\frac{D}{\sigma_{decay}}\right),$$

where D is the growth distance, $\tau_{decay} = 200$ s and $\sigma_{decay} = 3$ (normalized length) (Fig. 3 *C*). The timescale of GEF activation (τ_{decay}) was estimated from that of the NGF-induced activations of Cdc42 and Rac (26).

Gradient detection

Chemoattractive cue molecules ($n = 200{,}000$) were spatially distributed in a Gaussian form with a center at (0,0) and a standard deviation of 70. The actual number of floating cue molecules is thought to be large (32). Signal detection by moving filopodia and the reactions between membrane receptors and cue molecules are stochastic events. We approximated these situations in our model using stochastically generated molecules of a stationary density.

Resultant growing traces of the model growth cones are shown in Fig. 4. Model growth cones at various starting points successfully detected a chemoattractive gradient (Fig. 4, *A–C*). Model growth cones starting from (−70,−70) grew with various courses toward a path that was at 45° angle to the positive *x* axis (Fig. 4 *A*). This variability in the paths of the growth cones was due to the randomness of both the initial direction the growth cones' migrations and the distribution of the cue molecules. Similarly, model growth cones starting from (70,−70) grew toward a path that was at a 45° angle to the positive *x* axis (Fig. 4 *C*). Model growths cone starting from (−50,−50) also grew toward a path that was at a 45° angle to the positive *x* axis (Fig. 4 *B*). Additionally, the growth traces fanned out randomly when no cue gradient was supplied (Fig. 4 *D*).

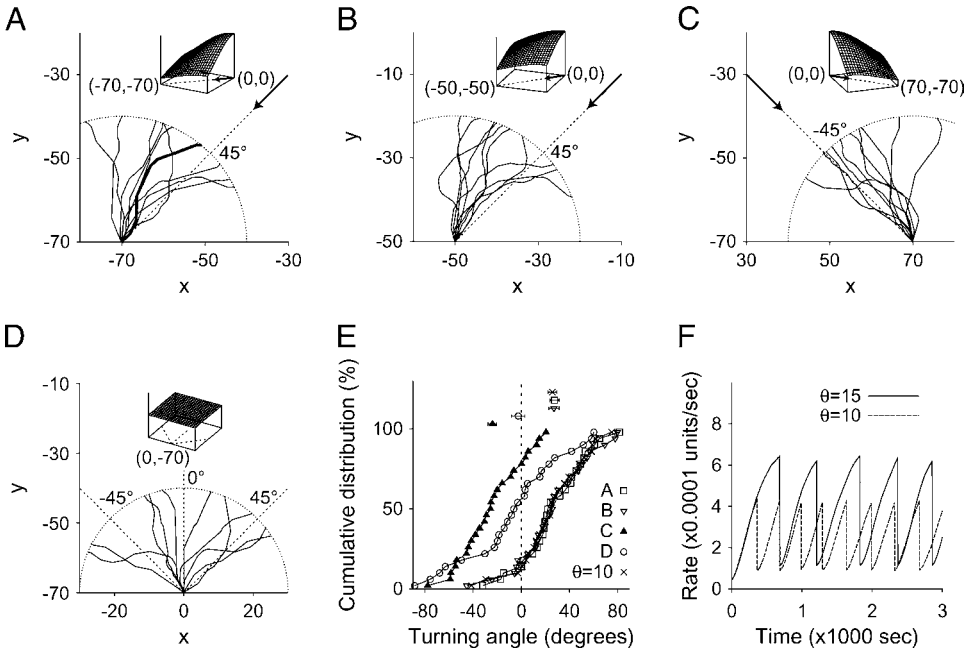

FIGURE 4 Chemoattractive guidance of model growth cones. (*A*) Traces of 10 model growth cones. All growth cones started from (−70,−70). The inset shows the density function of the cue molecules, the dotted circle has a radius of 30, and the dotted line indicates the direction of the distribution center. The angle is measured clockwise from the positive *y* axis. The initial direction was probabilistically determined by a Gaussian distribution whose central direction is the positive *y* axis with a standard deviation of 18°. (*B* and *C*) Same as panel *A* but the starting points of the growth cones are (−50,−50) and (+70,−70), respectively. (*D*) Same as panel *A* but the starting point of the growth cones are (0,−70) and the cue molecules are uniformly distributed within the *x* and *y* ranges of [−80:80] and [−90:10]. (*E*) Cumulative distributions of the turning angles of the model growth cones measured 30 units away from the starting points in panels *A–D*. The distribution with a low threshold ($\theta = 10$) is also shown. The top five points indicate the mean angle (±SE) for each condition (50 traces). (*F*) The growth rates for the thick line in panel *A* (*solid line*) and a low threshold ($\theta = 10$, *dashed line*). After one of $G_{i,i+1}$ values reaches the threshold for a jumping expansion mode, the rate for the whole growth cone goes down rapidly.

Accuracy of the directions of growth is quantified in Fig. 4 *E* by examining the cumulative distributions of the turning angles. Five points at the top of the figure indicate the average turning angle with the standard error of mean (mean ± SE) for the cones shown in Fig. 4, *A–D*, (50 traces) and with a low threshold. If the threshold was set to a much lower value ($\theta = 2$), the growth cone turned very frequently and lost efficient guidance. Average turning angles were the largest and smallest in the conditions used in Fig. 4, *A* and *C*, respectively. Average turning angle of the growth cones in Fig. 4 *B* was almost the same as that in Fig. 4 *A*, whereas the average turning angle of the growth cones in Fig. 4 *D* was almost zero. Growth cone had the ability of gradient detection even when the threshold value was multiplied by 2/3 (Fig. 4 *E*). Sole characteristic difference was that the growth cone tended to turn more frequently with a low threshold (*dashed line* in Fig. 4 *F*) and to extend along a straight path with a high threshold.

The model growth cones showed zigzag traces (Fig. 4, *A–D*) and an intermittent motility (Fig. 4 *F*). Experimental observations supporting our simulation results have been made; developing growth cones exhibit a zigzag trajectory when growing toward a chemoattractant source (25), and stop-and-move behaviors (9).

The model growth cone grew within a restricted distribution range when external molecules were distributed in a specific range (Fig. 5 *A*). The model growth cone also extended and turned at a densely distributed horizontal band of the external cues (Fig. 5 *B*). Such restricted or biased distributions of external cue molecules and axons growing along these distributions have been observed (33). Moreover, the model growth cone without a switching function (*linear model 1* in Fig. 3 *B*) could not detect the gradient because all of the lamellipodia remained in the normal expansion mode (Fig. 5 *C*). Such insensitivity to the gradient was also observed when a linear expansion rate function with a steeper slope (*linear model 2* in Fig. 3 *B*) was used. Even when the spatial diffusion of exogenous GEF was small ($G_{i,i+1} = (K_i + K_{i+1})/2 + G$), growth cones without switching did not detect a gradient but extended in straight lines (almost the same as in Fig. 5 *C*, data not shown), because localized GEF signals generate equal expansion due to linear activation (Fig. 3 *B*), despite the enhancement of signal localization (weak diffusion). Our results show that by using a switching mechanism for GTPase activities, the model growth cone requires a nonlinear system rather than signal localization to detect an external chemoattractive gradient.

Reaction coefficients for oscillation

The model shown in Fig. 1 *B* assumed that there are six pathways that allow cross talk between three GTPases, two of which are experimentally known (Cdc42 → Rac and Rac → Rac (34). The other four pathways have not yet been experimentally confirmed. To clarify the plausibility of the hypothetical signaling cascades drawn in Fig. 1 *B*, we examined which cascade was significant for the switching

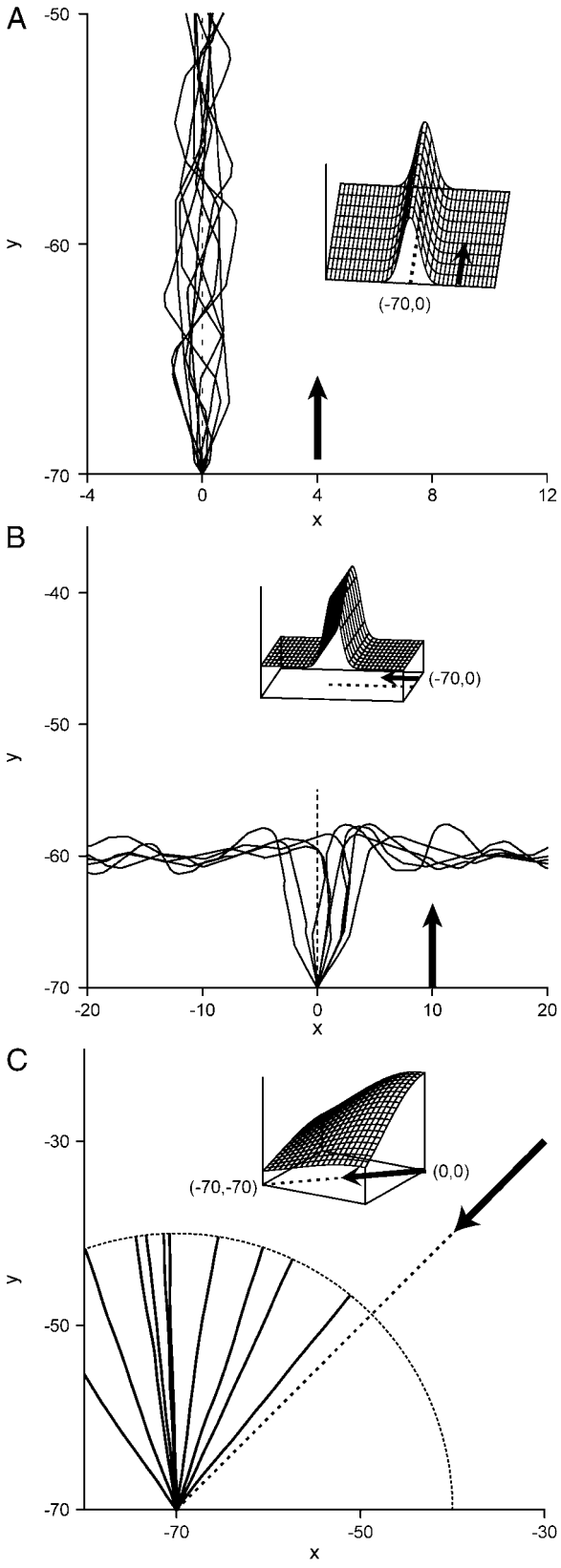

FIGURE 5 Chemoattractive guidance of model growth cones, responding to specific cue distributions (*A* and *B*) or without the switching function (*C*). (*A*) Cue molecules are distributed in a vertical Gaussian band ($n = 1250$, $[-90{:}10]$ along the y axis and $N(0,3)$ along the x axis, where $N(c, s)$ denotes a Gaussian distribution with a center, c, and a standard deviation, s). (*B*) Cue molecules are distributed in a horizontal Gaussian band ($[-80{:}80]$ along the x axis, $N(-60,3)$ along the y axis, and $n = 2000$) overlying a uniform distribution of the cue ($[-80{:}80]$ along the x axis, $[-90{:}10]$ along the y axis, and $n = 10,000$). (*C*) Same as Fig. 4 *A* but the switching function is removed by employing the function linear 1 from Fig. 3 *B*.

responses of all three GTPases by varying the kinetics parameters (Eqs. 4–6). The distributions of the allocation count of a random parameter set for realizing GTPase switching (oscillation and convergence) are shown in Fig. 6. We examined the original kinetics (Fig. 6 *A*) and the six deficient conditions, each of which lacked one of the six pathways (Fig. 6, *B–G*). When the distribution was biased to small allocation counts, the absent cascade was not very important for the GTPase switching response. On the contrary, the distributions that were biased to large allocation counts revealed the importance of the absent cascade for switching. The results suggest that GTPase switching response requires four unconfirmed signaling cascades: the inhibition of RhoA by Cdc42 (Fig. 6 *D*), the activation of RhoA by Rac (Fig. 6 *E*), and the inhibitions of Cdc42 and Rac by RhoA (Fig. 6, *F* and *G*, respectively). We suggest that these chemical pathways should exist if growth cones are able to detect a cue gradient using switching activations of the GTPases.

DISCUSSION

What is the role of the oscillating amount of activated GTPase? As mentioned above, the oscillation provokes efficient polymerization of actin filaments and enables some filopodia and lamellipodia to expand more effectively. Otherwise, all filopodia and lamellipodia would expand at a similar rate. Thus, the cross talk between the Rho-family G-protein functions as a winner-takes-direction system with a spatiotemporal integration of the external signals. Moreover, ultrasensitive switching has been observed in various other chemical reactions (35). Without the winner-takes-direction function, the model growth cone cannot detect the gradient of guidance cue molecules and its growing trace was a nearly straight line (Fig. 5 *C*). This result implies that the nonlinear switch produced by the GTPase cross talk is essential for gradient detection, and that the ultrasensitive oscillation is used when growth cones change their growing directions dramatically.

Bacteria, which possess no filopodia, use actin-based motility, but the motility mechanism differs from that of a growth cone (36). Growth cones follow the direction of an external gradient by changing their shape (corresponding to the jumping-expansion mode) and by repeating stop and go behaviors, whereas bacteria detect a gradient by comparing concentrations at two receptor points on a cell and by actively rotating instead of changing their shape. The movements of filopodia precede those of a growth cone, and to offset

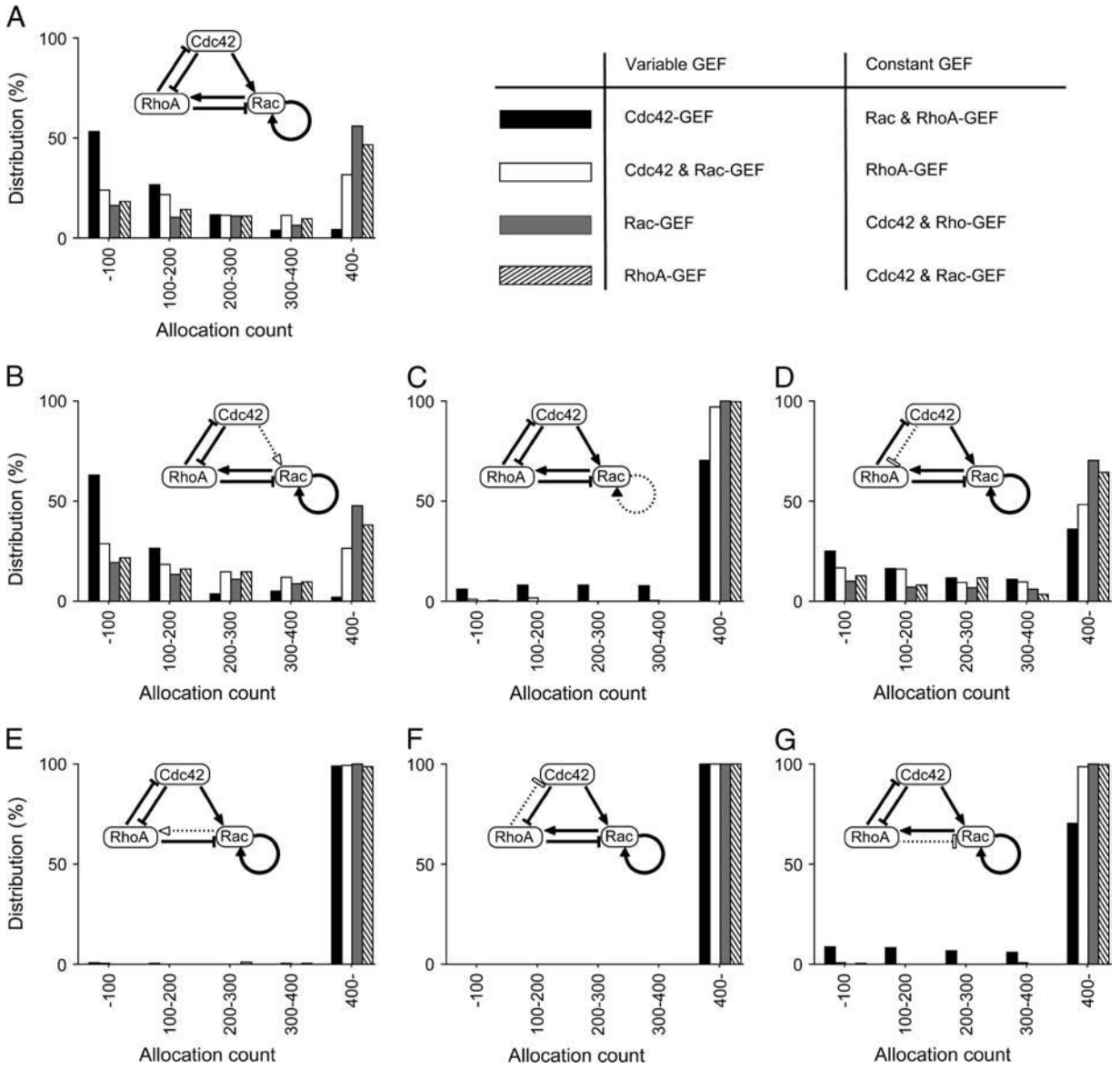

FIGURE 6 Distributions of the switching parameter allocation count. Distributions were computed as the percentages of parameter sets (out of 300 Monte Carlo allocations), with which the GTPase kinetics showed switching responses between convergence and spontaneous oscillation when exogenous GEF concentration varied in the range of [0.01:0.30] and the concentrations of other GEFs were held constant (0.01) (see *top right* table). The parameter values are randomly selected from $j/100, (j = 1, \cdots, 30)$ for inverse constant of dissociation, $j/100, (j = 1, \cdots, 50)$ for Michaelis constant, and $i/10, (i = 1, \cdots, 9)$ for catalytic constants. The counting process is as follows: 1), Allocate random values in reaction parameters. 2), Calculate the kinetics to draw the GTPase response curve (Fig. 2 *A*). Note that one or two exogenous GEF(s) are varied and the others are fixed to 0.01 in this calculation. 3), Count up if the GTPase response curve exhibits switching from oscillation to convergence. If the GTPase activities converge, increment the allocation count by one and return to step 1. 4), Repeat steps 1–3 300 times. (*A*) Original signal cascade of GTPase cross talk. (*B*) The activation of Rac by Cdc42 is removed ($k_1 = 0$). (*C*) The self-activation of Rac is removed ($l_1 = 0$). (*D*) The inhibition of RhoA by Cdc42 is removed ($k_2 = 0$). (*E*) The activation of RhoA by Rac is removed ($l_2 = 0$). (*F*) The inhibition of Cdc42 by RhoA is removed ($m_1 = 0$). (*G*) The inhibition of Rac by RhoA is removed ($m_2 = 0$).

the small growth-cone body, filopodia work to enhance gradient detection by a scouting mechanism. Conversely, gradient detection by cells that lack filopodia relies on feedback that results from the motility of the cell. These gradient detection methods are essentially the same in that they measure concentration differences of an extracellular molecule. Growth cones, however, have developed an efficient detection mechanism using filopodia but are restricted in that they are always connected to microtubules and cannot move freely.

In the previous theoretical studies (6,7), model cells could detect an external cue gradient by self-amplifying small differences in the gradient and globally inhibiting other parts of the cell. These models explained the sensitivity of cells to the external cue gradient without cell movement or changes

in cell morphology. In the previous studies, global inhibitor molecules such as PTEN were modeled to diffuse inside of the whole cell (7) and the external cue gradient was assumed to be spatially smooth and continuous. In our model, on the other hand, we have assumed that the actin polymerization is globally inhibited because the distribution of the actin monomers is locally biased in the model growth cone, i.e., in the area where Cdc42 and Rac GTPases have extremely high activities. In addition, the external cue molecules have been modeled to be discretely distributed, so that the local cue gradient is no longer smooth. Our model growth cone was able to discount the locally rough gradient and used axonal movements to detect the global cue gradient by spatiotemporal integration of the signal. For the GTPase activation, it is possible that Cdc42 and Rac are activated by a feedback loop downstream of PI3K activation (7). In this study, we have attempted to show the possible function of the cross talk between the GTPases in detecting the cue gradient for axon guidance. Moreover, our assumption that the extreme activation of Rac produces a new growth cone may be the molecular foundation underlying recent theoretical studies about the generation of new filopodia (8).

In our model, the concentration of an exogenous GEF (C_{GEF}) has been introduced as a controlling parameter for axonal guidance. Of the other exogenous GEFs, RhoA-GEF (H_{GEF}) tends to suppress the GTPase oscillations because active RhoA inhibits the activations of both Cdc42 and Rac. It is likely that such suppression of GTPase oscillation would induce repulsive turning during axon elongation. When the GTPase kinetics are implemented into the model growth cone, six exogenous parameters, a GEF and a GAP for each of the three GTPases, may reproduce the complicated behaviors of axonal elongation. Our study has revealed that the GTPase cross talk shows a nonlinear response to external signals, which could be crucial for nonlinear movements of the growth cone, whereas there is a possibility that another nonlinearity such as protein recruitment by actin filaments at a downstream step (37) works as a switching-like system. Actually, a nonlinear process has been observed upstream (38): transient pulses of phosphatidylinositol 3-phosphate (PI3P), a product of phosphatidylinositol 3-kinase (PI3K). A positive feedback loop including PI3K and GTPases has been also reported (21,39,40).

Using computer simulations, we have shown that the morphological changes of a growth cone (physical behavior), gradient detection by extending axons, and axonal guidance (biological function) can be explained by interactions between activated GTPases (chemodynamic reaction). Although based on a number of assumptions, our approach provides one potential way to integrate and unify molecular interactions and biological phenomena beyond chemodynamics.

Many factors other than G-proteins affect the motility of growth cones in axon guidance. Adhesion molecules such as integrins or cadherins influence the motility of growth cones (41). It has also been observed that protein synthesis is involved in axon guidance (32), and the possibility of protein synthesis at a growth cone has been examined (42). To further clarify the mechanisms underlying axonal guidance, these factors should be included in future work.

We thank Mu-Ming Poo for valuable suggestions.

This work was supported by a Grant-in-Aid for Scientific Research 16014214 and by Special Coordination Funds Promoting Science and Technology (both from the Japanese Ministry of Education, Culture, Sports, Science, and Technology), and by the Inamori Foundation.

REFERENCES

1. Sperry, R. W. 1963. Chemoaffinity in the orderly growth of nerve fiber patterns and connections. *Proc. Natl. Acad. Sci. USA*. 50:703–710.
2. Tessier-Lavigne, M., and C. S. Goodman. 1996. The molecular biology of axon guidance. *Science*. 274:1123–1133.
3. Pantaloni, D., C. L. Clainche, and M. F. Carlier. 2001. Mechanism of actin-based motility. *Science*. 292:1502–1506.
4. Grunwald, I. C., and R. Klein. 2002. Axon guidance: receptor complexes and signaling mechanisms. *Curr. Opin. Neurobiol*. 12:250–259.
5. Dickson, B. J. 2002. Molecular mechanisms of axon guidance. *Science*. 298:1959–1964.
6. Meinhardt, H. 1999. Orientation of chemotactic cells and growth cones: models and mechanisms. *J. Cell Sci*. 112:2867–2874.
7. Levchenko, A., and P. A. Iglesias. 2002. Models of eukaryotic gradient sensing: application to chemotaxis of amoebae and neutrophils. *Biophys. J*. 82:50–63.
8. Goodhill, G. J., M. Gu, and J. S. Urbach. 2004. Predicting axonal response to molecular gradients with a computational model of filopodial dynamics. *Neural Comput*. 16:2221–2243.
9. Kalil, K., G. Szebenyi, and E. W. Dent. 2000. Common mechanisms underlying growth cone guidance and axon branching. *J. Neurobiol*. 44:145–158.
10. Polinsky, M., K. Balazovich, and K. W. Tosney. 2000. Identification of an invariant response: stable contact with Schwann cells induces veil extension in sensory growth cones. *J. Neurosci*. 20:1044–1055.
11. Luo, L. 2000. Rho GTPases in neuronal morphogenesis. *Nat. Rev. Neurosci*. 1:173–180.
12. Dickson, B. J. 2001. Rho GTPases in growth cone guidance. *Curr. Opin. Neurobiol*. 11:103–110.
13. Bray, D. 1995. Protein molecules as computational elements in living cells. *Nature*. 376:307–312.
14. Ridley, A. J., and A. Hall. 1992. The small GTP-binding protein Rho regulates the assembly of focal adhesions and actin stress fibers in response to growth factors. *Cell*. 70:389–399.
15. Giniger, E. 2002. How do Rho family GTPases direct axon growth and guidance? A proposal relating signaling pathways to growth cone mechanics. *Differentiation*. 70:385–396.
16. Liebl, E. C., D. J. Forsthoefel, L. S. Franco, S. H. Sample, and J. E. Hess. 2000. Dosage-sensitive, reciprocal genetic interactions between the Abl tyrosine kinase and the putative GEF trio reveal trio's role in axon pathfinding. *Neuron*. 26:107–118.
17. Bateman, J., H. Shu, and D. V. Vactor. 2000. The guanine nucleotide exchange factor trio mediates axonal development in the Drosophila embryo. *Neuron*. 26:93–106.
18. Etienne-Manneville, S., and A. Hall. 2002. Rho GTPases in cell biology. *Nature*. 420:629–635.
19. Hu, H., T. F. Marton, and C. S. Goodman. 2001. Plexin B mediates axon guidance in *Drosophila* by simultaneously inhibiting active Rac and enhancing RhoA signaling. *Neuron*. 32:39–51.

20. Zhang, B., J. Chernoff, and Y. Zheng. 1998. Interaction of Rac1 with GTPase-activating proteins and putative effectors. *J. Biol. Chem.* 273:8776–8782.

21. Shi, S. H., L. Y. Jan, and Y. N. Jan. 2003. Hippocampal neuronal polarity specified by spatially localized mPar3/mPar6 and PI3-kinase activity. *Cell.* 112:63–75.

22. Zhu, K., B. Debreceni, R. Li, and Y. Zheng. 2000. Identification of Rho GTPase-dependent sites in the Dbl homology domain of oncogenic Dbl that are required for transformation. *J. Biol. Chem.* 275:25993–26001.

23. Maeda, M., S. Lu, G. Shaulsky, Y. Miyazaki, H. Kuwayama, Y. Tanaka, A. Kuspa, and W. F. Loomis. 2004. Periodic signaling controlled by an oscillatory circuit that includes protein kinases ERK2 and PKA. *Science.* 304:875–878.

24. Bhalla, U. S., and R. Iyengar. 1999. Emergent properties of networks of biological signaling pathways. *Science.* 283:381–387.

25. Ming, G. L., H. J. Song, B. Berninger, C. E. Holt, M. Tessier-Lavigne, and M.-M. Poo. 1997. cAMP-dependent growth cone guidance by netrin-1. *Neuron* 19: 1225–1235.

26. Aoki, K., T. Nakamura, and M. Matsuda. 2004. Spatio-temporal regulation of Rac1 and Cdc42 activity during nerve growth factor-induced neurite outgrowth in PC12 cells. *J. Biol. Chem.* 279:713–719.

27. Ponti, A., M. Machacek, S. L. Gupton, C. M. Waterman-Storer, and G. Danuser. 2004. Two distinct actin networks drive the protrusion of migrating cells. *Science.* 305:1782–1786.

28. Edwards, D. C., L. C. Sanders, G. M. Bokoch, and G. N. Gill. 1999. Activation of LIM-kinase by Pak1 couples Rac/Cdc42 GTPase signalling to actin cytoskeletal dynamics. *Nat. Cell Biol.* 1:253–259.

29. Sumi, T., K. Matsumoto, Y. Takai, and T. Nakamura. 1999. Cofilin phosphorylation and actin cytoskeletal dynamics regulated by Rho- and Cdc42-activated LIM-kinase 2. *J. Cell Biol.* 147:1519–1532.

30. Lou, Z., D. D. Billadeau, D. N. Savoy, R. A. Schoon, and P. J. Leibson. 2001. A role for a RhoA/ROCK/LIM-kinase pathway in the regulation of cytotoxic lymphocytes. *J. Immunol.* 167:5749–5757.

31. Steketee, M. B., and K. W. Tosney. 2002. Three functionally distinct adhesions in filopodia: shaft adhesions control lamellar extension. *J. Neurosci.* 22:8071–8083.

32. Ming, G. L., S. F. Wong, J. Henley, X. Yuan, H. Song, N. C. Spitzer, and M.-M. Poo. 2002. Adaptation in the chemotactic guidance of nerve growth cones. *Nature* 417: 411–418.

33. Yamamoto, N., A. Tamada, and F. Murakami. 2003. Wiring of the brain by a range of guidance cues. *Prog. Neurobiol.* 68:393–407.

34. Bagrodia, S., and R. A. Cerione. 1999. PAK to the future. *Trends Cell Biol.* 9:350–355.

35. Hardie, D. G., I. P. Salt, S. A. Hawley, and S. P. Davies. 1999. AMP-activated protein kinase: an ultrasensitive system for monitoring cellular energy charge. *Biochem. J.* 338:717–722.

36. Goodhill, G. J., and J. S. Urbach. 1999. Theoretical analysis of gradient detection by growth cones. *J. Neurobiol.* 41:230–241.

37. Wedlich-Soldner, R., S. Altschuler, L. Wu, and R. Li. 2003. Spontaneous cell polarization through actomyosin-based delivery of the Cdc42 GTPase. *Science.* 299:1231–1235.

38. Arrieumerlou, C., and T. Meyer. 2005. A local coupling model and compass parameter for eukaryotic chemotaxis. *Dev. Cell.* 8: 215–227.

39. Weiner, O. D., P. O. Neilsen, G. D. Prestwich, M. W. Kirschner, L. C. Cantley, and H. R. Bourne. 2002. A PtdInsP(3)- and Rho GTPase-mediated positive feedback loop regulates neutrophil polarity. *Nat. Cell Biol.* 4:509–513.

40. Cheng, T. L., M. Symons, and T. S. Jou. 2004. Regulation of anoikis by Cdc42 and Rac1. *Exp. Cell Res.* 295:497–511.

41. Rhee, J., N. S. Mahfooz, C. Arregui, J. Lilien, J. Balsamo, and M. F. VanBerkum. 2002. Activation of the repulsive receptor Roundabout inhibits N-cadherin-mediated cell adhesion. *Nat. Cell Biol.* 4: 798–805.

42. Steward, O. 2002. Translating axon guidance cues. *Cell.* 110: 537–540.